

Compressive Strength Prediction for Industrial Waste-Based SCC Using Artificial Neural Network

Md. Akram Hossain¹, G. M. Sadiqul Islam^{2*}, Amit Mallick¹

¹Graduate, Department of Civil Engineering, Chittagong University of Engineering and Technology
Kaptai Road, Chattogram-4349, Bangladesh

²Professor, Department of Civil Engineering, Chittagong University of Engineering and Technology
Kaptai Road, Chattogram-4349, Bangladesh

*Corresponding author: gmsislam@cuet.ac.bd

SUBMITTED 23 February 2022 **REVISED** 7 July 2022 **ACCEPTED** 15 August 2022

ABSTRACT Concrete is the most used construction material in the world. Sustainable construction practice demands durable material. A particular type of concrete that flows and consolidates under its weight is proposed to reduce labor dependency during construction, called self-compacting concrete. It is installed without vibration due to its excellent deformability and flowability while remaining cohesive enough to be treated without difficulty. Evaluating its compressive strength is essential as it is used in important construction projects. An artificial neural network (ANN) is a predicting tool that can predict output in various sectors. This study evaluated the compressive strength of industrial waste such as fly ash and silica fume incorporated in self-compacting concrete at various ages. A non-linear relationship was used to develop the model relating mix composition and SCC compressive strength using an Artificial Neural Network (ANN). The experimental and expected outcomes were compared with the model prediction to evaluate the predictive capacity, generalize the generated model, and observe suitable matches. The developed ANN network can predict the desired output, i.e., compressive strength incorporating industrial waste. Furthermore, the influence of individual parameters viz. cement, silica fume, and fly ash, w/b were also evaluated using parametric analysis, which shows the sensitivity of various materials on the compressive strength of Self-compacting concrete. As a result, a higher correlation coefficient of 0.9835 with a smaller value of MAPE (0.0347) and RMSE (2.4503) is obtained. Finally, a process of creating tools for practical engineers and field users is proposed, which would be very handy and fast for predicting the strength of SCC.

KEYWORDS Self-compacting concrete; Industrial Waste; Artificial Neural Network; Back-propagation; Fly ash

© The Author(s) 2023. This article is distributed under a Creative Commons Attribution-ShareAlike 4.0 International license.

1 INTRODUCTION

Concrete has been used as a construction material for over a century and has been continuously developed as indicated by the increased usage of secondary cementitious elements in the binding phase (Heniegal, 2012; Neville, 2011). Moreover, self-compacting concrete (SCC) is normally installed without any outward vibration and has revolutionized concrete technology due to its self-flow and self-compaction ability (Okamura and Ouchi, 2003; Raheman and Modani, 2013). It is different from ordinary concrete in some random cases based on its properties such as the high workability as well as higher water and fine content requirement. It is important to note that there has been meaningful improvement in the study related to this concrete since its develop-

ment (Siddique, 2011). Self-compacting concrete can be produced using industrial wastes such as fly ash, ladle slag, silica fume, and others. Fly ash and silica fume are frequently used because they provide extended durability for construction projects (Deilami et al., 2017; Joshi and Lohtia, 1997; Mazloom et al., 2018). Moreover, the property enhancement of concrete at different curing states using these industrial by products has been documented with a special focus on the benefits of long-term water curing (McCarthy et al., 2013). The effect of SCMs on the properties of SCC has been studied as observed with fly ash (Intezar et al., 2019), silica fume (Turk et al., 2012), and GGBS (Saini and Vattipalli, 2020). Plastic fibers (Al-Hadithi and Hilal, 2016; Mohammad-

hosseini and Yatim, 2017) and steel fibers (Banthia and Onuaguluchi, 2021; Grünewald and Walraven, 2001) have also been used in SCC production. It was observed that there is a non-linear relationship between mixing constituents and compressive strength but there is no theoretical or mathematical relationship between mixture ratio and SCC strength (American Concrete Institute, 2019; Siddique et al., 2008). This means it is necessary to use appropriate methods to predict SCC strength based on the mixing ingredients during the design phase. One of the tools proposed to be useful in making this prediction is the Artificial Neural Network (ANN) (Taylor, 1992; Yadollahi et al., 2015). This is a flexible computer method to create examples or data based on the neural system of a human being. It has become increasingly popular and is currently being used in several engineering fields (Ashteyat and Ismeik, 2018; Taylor, 1992; Ye et al., 2019). Neural network model has the ability to predict more specific concrete properties while reducing the experimental work required in the laboratory or study center and on-site. The primary advantage of neural network model is that it does not need any specific equations because it is based only on learning and understanding input-output connections for any complicated problem.

This study aims to develop an ANN model in the form of optimum BPNN architecture and tools for practical engineers to reliably predict the SCC strength at multiple ages. The SCC used was produced through the application of industrial wastes such as silica fume and fly ash as a partial substitute for cement. Moreover, the model developed was used to assess the effect of individual parameters such as w/b ratio, cement, superplasticizer, and others on SCC's strength.

2 METHODOLOGY

The prediction of the SCC strength using an ANN required many reliable data or information on mix design and compressive strength. It is important to note that more accurate data usually leads to more reliable prediction and this is the reason the data used were obtained from available literature and in-house experimental results which were subsequently used to develop the network model. Moreover, the development cycle of the model was separated into three primary segments and these include the central which fo-

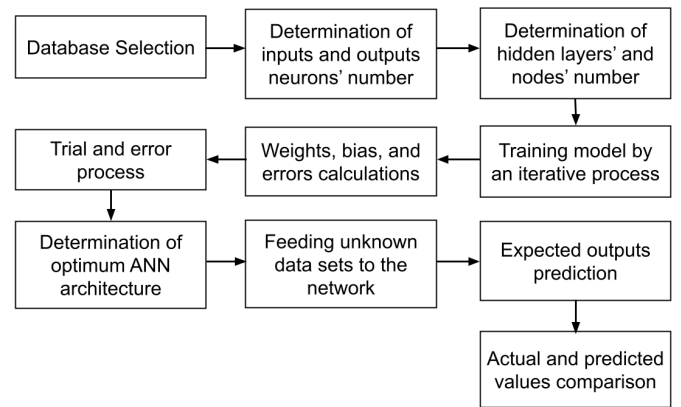


Figure 1. Flow diagram of the ANN development process focuses on gathering and analyzing SCC data with attention placed on fly ash and silica fume only. The second section focuses on determining different training parameters such as execution duration, performance function, learning method, and appropriate neural network model. The third and final section involves the approval of the proposed ANN models and the determination of their performances through the comparison with other available test data. The flow diagram of the overall process is provided in the following Figure 1.

2.1 Available literature

ANN is a prediction tool widely used in recent times to predict desired output in different sectors. It has been used very effectively in civil engineering and this is based on its ability to learn from experimental or analytical/theoretical data. ANN models have the ability to classify data, predict values, and assist in decision-making analogous to a response surface technique. Moreover, a trained ANN can produce more trustworthy findings with far less processing work compared to traditional numerical analysis processes such as regression analysis (Asteris et al., 2019a; Hornik et al., 1989). The functioning of ANN is similar to the human brain's organic neural network (Hinton et al., 2006; Schmidhuber, 2015). Its most fundamental component are the artificial neurons that receive inputs to produce an output after a mathematical function processing just like the biological neurons. It is pertinent to state that weights are usually assigned to the input parameters before the data reaches the neuron to replicate the biological neuron's unpredictable nature.

Table 1. Mix proportions of SCC

W/B	C (kg)	FA (kg)	SF (kg)	FnA (kg)	CA (kg)	SP (kg)	VMA (kg)	Age (Days)	f_c (Mpa)	Reference
0.33	500	0	0	984	656	6.5	0	28	65	
0.33	450	0	50	959	656	9.5	0	28	75.5	
0.33	400	0	100	935	656	12	0	28	79.5	
0.33	450	50	0	966	656	5.5	0	28	67	
0.33	400	100	0	948	656	4	0	28	80.5	
0.33	450	0	50	959	656	9.5	0	90	73	
0.33	450	50	0	966	656	5.5	0	90	73	
0.33	400	100	0	948	656	4	0	90	79.5	
0.33	450	0	50	959	656	9.5	0	180	79.5	
0.33	400	0	100	935	656	12	0	180	87	(Sabet et al., 2013)
0.33	450	50	0	966	656	5.5	0	180	79.5	
0.33	400	100	0	948	656	4	0	180	87	
0.35	467.5	82.5	0	677	677	5.3	0	28	45	
0.35	385	165	0	665	665	5.3	0	28	42	
0.35	522.5	0	27.5	684	684	6.4	0	28	53	
0.35	495	0	55	680	680	6.4	0	28	54	
0.35	412.5	82.5	55	669	668	6.2	0	28	47	
0.35	357.5	165	27.5	661	661	5.6	0	28	43	
0.35	330	165	55	657	657	5.6	0	28	43	
0.38	444	0	0	1010	777	4.44	0	28	53.8	
0.38	421.8	0	22.2	1002	777	5.328	0	28	63	
0.38	399.6	0	44.4	994	777	6.66	0	28	63.8	
0.38	377.8	0	66.2	986	777	6.66	0	28	72.1	(Behfarnia & Farshadfar, 2013)
0.38	444	0	0	1010	777	4.44	0	90	57	
0.38	421.8	0	22.2	1002	777	5.328	0	90	68	
0.38	399.6	0	44.4	994	777	6.66	0	90	67	
0.38	377.8	0	66.2	986	777	6.66	0	90	71.5	
0.35	500	0	0	967	694	8	0	28	78.5	
0.35	475	0	25	958	687	8	0	28	78.5	
0.35	450	0	50	954	685	9	0	28	82.5	
0.35	425	0	75	948	681	10	0	28	87	(Bingöl & Tohumcu, 2013)
0.35	375	125	0	938	673	7.5	0	28	61.5	
0.35	300	200	0	923	663	7.5	0	28	55	
0.35	225	275	0	908	652	7.5	0	28	43	
0.44	350	0	35	960	920	2.76	0	7	21.1	
0.44	350	0	35	960	920	2.76	0	28	26.1	(Faez et al., 2020)
0.44	350	0	35	960	920	2.76	0	90	29.3	
0.41	465	85	0	910	590	10.73	0	7	29.55	
0.41	440	110	0	910	590	11.01	0	7	27.99	
0.42	415	135	0	910	590	9.91	0	7	25.52	
0.43	385	165	0	910	590	9.91	0	7	23.98	
0.41	440	110	0	910	590	11.01	0	28	33.15	
0.42	415	135	0	910	590	9.91	0	28	31.47	(Siddique, 2011)
0.43	385	165	0	910	590	9.91	0	28	30.66	
0.44	355	195	0	910	590	9.91	0	28	29.62	
0.41	465	85	0	910	590	10.73	0	90	58.99	
0.42	415	135	0	910	590	9.91	0	90	43.77	
0.44	355	195	0	910	590	9.91	0	90	40.88	

ANN has been applied in different aspects of structural engineering as indicated by its usage in relation to different properties of concrete such as the creep and shear strength (Asteris et al., 2019b; Hodhod et al., 2018), cement-based mortar's strength (Asteris et al., 2019a), SCC's tensile strength (Mazloom and Yoosefi, 2013), and also to monitor the structural health (Ye et al., 2019) and durability of civil infrastructures.

2.2 Experimental dataset

An extensive and trustworthy dataset is required for any ANN to function properly. This means a comprehensive range of experimental data is necessary to determine the connection between the mixing elements of SCC and its observed characteristics. Meanwhile, it is hard for a single researcher to fully generate enough experimental data to train ANN. Another difficulty is the accuracy of accessible data because the database trains the optimal developed network, thereby leading to the failure of the trained network to predict proper values when inaccurate data or information are used. This is mainly due to the fact that a tiny group of inaccurate data can damage a larger volume of data. Table 1 shows the dataset utilized in the proposed ANN model with a portion observed to have been generated from the information published earlier in the institution's laboratory. They were organized based on nine input parameters which include silica fume, fly ash

and cement content, w/b ratio, coarse aggregates, fine aggregates, viscosity modifying agent (VMA), superplasticizer, and age of testing. However, the single output variable is the compressive strength of SCC.

A database of 354 mixtures was collected from the literature with similar physical and chemical characteristics. The requirements for the data identification were defined by the omission of a few SCC characteristics in some literature and the uncertainty of testing procedures and combination proportions. Moreover, the values acquired experimentally were earlier compared with the predicted results produced by the neural network. A pair of input and output vectors were used to train the ANN. The input vector contained mixed variables in the network model while the output vector had only one element which is the compressive strength. Most previous studies created databases based on their experimental results, thereby limiting their findings to their immediate environment. However, the database for this study was obtained from different sources including literature from multiple countries to have a broader range of situations. The boundary values of variables used to develop the model are presented in Table 2 while the range and distribution of the input and output variables are indicated in Table 3.

Table 2. Ranges of input and output variables

Constituents	Min.	Max.	Avg.
Input variables			
Water/binder	0.3	0.45	0.37
Cement (kgm^{-3})	135	600	356.94
Silica fume (kgm^{-3})	0	150	22.61
Fly ash (kgm^{-3})	0	420	124.97
Fine agg. (kgm^{-3})	657	1166	908.46
Coarse agg. (kgm^{-3})	590	1000	731.27
Superplasticizer (kgm^{-3})	0.585	13.8	5.31
VMA (kgm^{-3})	0	4.03	0.1
Age (days)	7	180	40.92
Output variable			
Compressive strength (MPa)	17.7	106.6	56.47

Table 3. Distribution of inputs variables in the database

W/B		Cement		Fly ash	
Range (kgm^{-3})	Ferq.	Range (kgm^{-3})	Ferq.	Range (kgm^{-3})	Ferq.
0.25-0.31	42	100-250	91	0-115	183
0.32-0.38	160	251-400	128	116-230	87
0.39-0.44	120	401-550	119	231-345	69
0.45-0.5	32	551-700	16	346-460	15
Silica fume		Fine aggregates		Coarse aggregates	
0-40	261	650-790	78	550-675	171
41-80	78	791-930	107	676-800	68
81-120	92	931-1070	135	801-925	97
121-160	1	1071-1200	34	926-1050	18
Superplasticizer		VMA		Ages (days)	
0.5-3.87	159	0-1.125	348	7	91
3.88-7.25	64	1.126-2.25	0	28	170
7.26-10.63	104	2.251-3.375	0	90	85
10.64-14	27	3.376-4.5	6	180	8

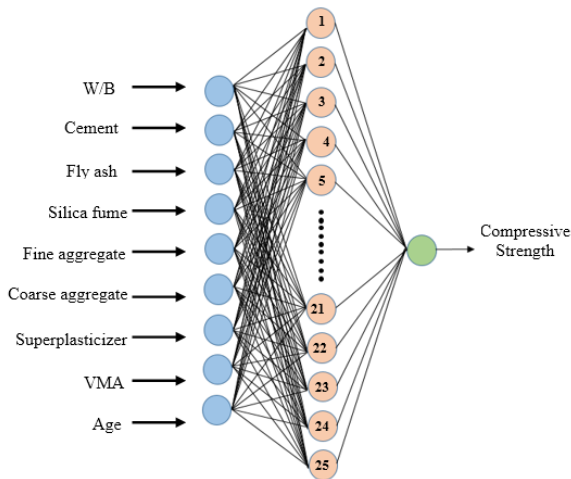


Figure 2. Visual representation of the variables in the model developed

2.3 Development of model

The variables influencing concrete strength were used to calculate the number of input neurons. It was difficult to develop the training architecture in a reasonable amount of time due to the existence of too many factors which also makes it impractical from the engineering perspective that permits a $\pm 10\%$ error margin. Therefore, all conceivable variables were considered during the early development stage and this led to the usage of nine variables as the fundamental input neurons in the proposed model as indicated in Figure 2.

Concrete strength generally increases with curing age and this is the reason 28-day compressive strength is a good indicator of design quality and control. Meanwhile, the initial strength within 7-days after placing is critical in determining the ability of concrete to handle disposal and shoring reduction. This is the reason the concrete strength was measured at four distinct ages. The primary number of output neurons was considered one and utilized for the proposed model because this study is interested in determining the compressive strength of SCC as an output. Different optimization methods were investigated to determine the optimum training algorithm and it was discovered that Levenberg-Marquardt (implemented by Levmar) offered the best ANN prediction for the output. This technique appears to be best for training feed-forward back-propagation neural network with non-linear issues that are moderately large (up to several hundred neurons per layer) (Lourakis, 2005). It is also significantly

Table 4. Training parameters of the BPNN model developed

Training parameters	Values
Training algorithm	Levenberg-Marquardt
Normalization	Min-Max (0.1-0.9)
Input neurons	9
Hidden layers	1
Hidden neurons	25
Output neurons	1
Training error goal	0
Performance function	MSE
Transfer function	Tansig & Purelin
Time	Infinite
Learning cycle	1000
Minimum gradient	1×10^{-7}
Maximum fail	6

MSE: Mean square error

Tansig: Hyperbolic tangent sigmoid transfer function

Purelin: Linear transfer function

different from the other methods due to its ability to train networks quickly in addition to its effectiveness on non-linear problems. The Levenberg-Marquardt method was used in the MATLAB software and this improved its capabilities because the MATLAB environment has the built-in function to solve matrix equations.

Several distinct BPNN models were designed and deployed in this study with 3 to 30 hidden neurons selected for the trial. Moreover, for every trialed model, the input and output neurons were kept at 9 and 1 respectively because the mixture contains 9 mix constituents with the SCC strength to be determined as earlier mentioned. The developed models were also expressed as NN 9-Y-1 with the hidden neuron indicated as Y and ranges from 3 to 30. First, the model was trained using 248 mix data out of 354 data pairs (70% of total data points). The validation and test was later conducted using the remaining 107 data pairs (30% of the complete pairs) such that 53 (15%) were used for the validation and 53 (15%) for the test (Apostolopoulou et al., 2019; Armaghani et al., 2019; Asteris et al., 2016; Cavaleri et al., 2017; Nikoo et al., 2017). The maximum allowable error was also calculated using the rule described in the previous literature (Lee et al., 2001; Lee and Han, 2002). All the parameters employed in the training are presented in Table 4.

Table 5. Coefficients of the optimum proposed neural network model

BPNN Model	9-24-1		9-25-1		9-26-1		9-27-1		9-28-1		9-29-1	
	R ²	RMSE										
Training	0.9807	3.1352	0.9912	1.7464	0.9823	2.5768	0.9922	1.7233	0.9948	1.4035	0.9851	2.3366
Validation	0.8913	6.3150	0.9629	3.3227	0.9178	5.8728	0.9301	4.7212	0.9351	5.1613	0.9456	4.8445
Testing	0.9514	4.8713	0.9631	3.3211	0.9456	4.3829	0.9432	4.5210	0.9851	4.7371	0.9008	5.5462

Table 6. Coefficients of the optimum proposed neural network model

ANN model	R ²	MAPE	RMSE
9-25-1	0.9835	0.0347	2.4503

2.4 Performance evaluation

Several statistical indexes are normally applied to assess the performance of the neural network model but this study only used three including the root mean square error (RMSE), mean absolute percentage error (MAPE), and Pearson correlation coefficient (R²) which have been widely used and accepted (Chugh, 2020; Vandeput, 2019). The models with smaller RMSE and MAPE values usually have more exact predictions and those with higher R² values provide more correlated analytical and projected values. The following formulas were used to determine these parameters and the results are presented in Table 5 (Apostolopoulou et al., 2019).

$$RMSE = \sqrt{\frac{1}{n} \sum_{i=1}^n (actual_i - predicted_i)^2} \quad (1)$$

$$MAPE = \frac{1}{n} \sum_{i=1}^n \left| \frac{actual_i - predicted_i}{actual_i} \right| \quad (2)$$

$$R^2 = 1 - \left(\frac{\sum_{i=1}^n (actual_i - predicted_i)^2}{\sum_{i=1}^n (actual_i - actual)^2} \right) \quad (3)$$

Where, n is the total number of datasets.

3 RESULT AND DISCUSSION

The final goal of this study is to develop an optimum neural network model and design a tool for practical application. The acceptance of the model depends on its ability to predict the output effectively and this was determined through cross-validation which is normally applied to determine the accuracy of a developed model. Moreover, the input data pair was separated into multiple groups and each was used to evaluate a model that fits the remaining portion.

Statistical approaches are frequently employed to create empirical relationships between numerous interacting elements but the process is usually complicated and convoluted, specifically when dealing with non-linear relations. It requires knowing the critical parameters to create the statistical model. Meanwhile, back-propagation neural network have a more straightforward modeling procedure because no mathematical equation is needed for the input and output variables. This means ANN has the ability to assist study systems with several variables as well as to identify previously unknown patterns and features. The neural network is taught to handle noisy or imprecise data because they are trained on actual test data. Moreover, it is easy to update the model when new data becomes available by retraining using the latest data patterns.

The prediction of the strength of the SCC with industrial waste was conducted by developing and evaluating several BPNN models. A total of 26 distinct ANN architectures were specifically developed using one hidden layer while the indexes of the six ANN model cases developed are presented in Table 5. The optimal BPNN model 9-25-1 was selected based on its R² and RMSE values for the compressive strength prediction.

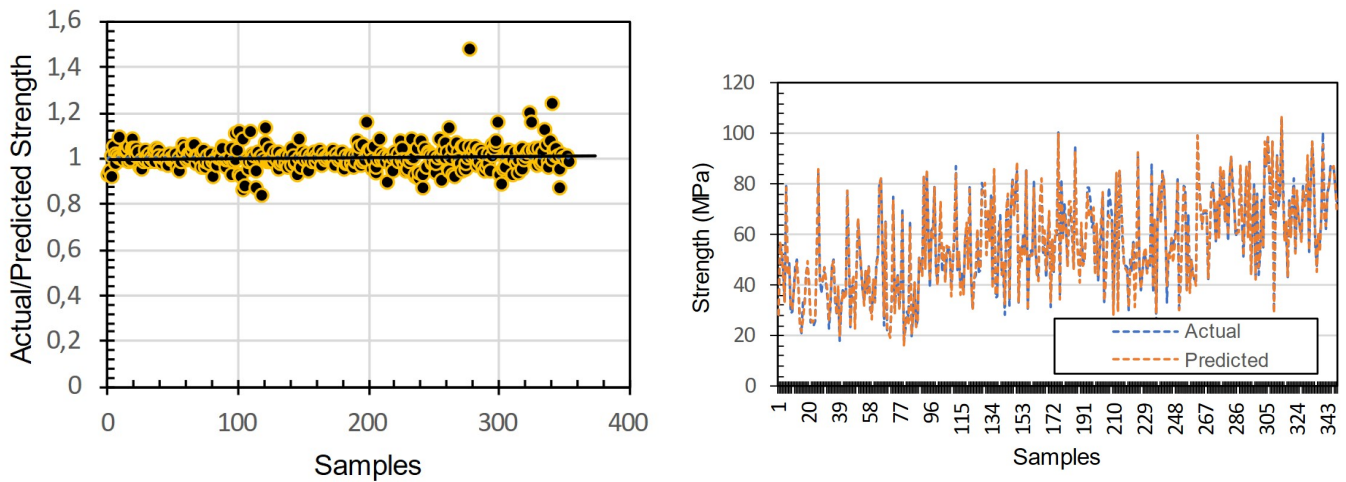


Figure 3. Actual vs predicted strength for the test dataset

Table 7. Actual and predicted strength (MPa) for testing data sets of ANN

Input variables								Output			
W/B	(kgm ⁻³)							Age, days	Actual Strength, MPa	Predicted Strength, MPa	E(%)
	Cement	Fly Ash	Silica fume	Fine agg.	Coarse agg.	SP	VMA				
0.30	620	0	0	740	775	8.06	4.03	7	47.1	46.33	1.63
0.31	589	0	31	740	775	8.06	4.03	7	56.5	56.52	0.03
0.31	573	0	47	740	775	8.06	4.03	7	60.1	60.27	0.28
0.30	620	0	0	740	775	8.06	4.03	28	60.2	60.72	0.87
0.31	589	0	31	740	775	8.06	4.03	28	73.1	72.63	0.64
0.31	573	0	47	740	775	8.06	4.03	28	76.3	77.46	1.53
0.35	154	309	51	980	621	2.056	0	7	40.5	40.06	1.09
0.32	220	247.5	82.5	685	880	8.89	0	90	68.3	69.32	1.50
0.39	220	180	0	916	900	1.4	0	28	45	46.69	3.76
0.30	540	0	60	1059	595	8.58	0	7	84.5	86.21	2.03
0.40	600	0	0	810	660	13.8	0.9	7	35	37.35	6.70
0.35	206	257	51	1001	621	2.57	0	7	48.2	47.97	0.47
0.35	327	173	0	902	803	4.42	0	28	61.6	61.16	0.71
0.45	371	159	0	768	668	0.86	0.082	28	41.4	40.01	3.35
0.40	510	0	90	810	660	13.8	0.9	28	55.3	55.06	0.44
0.40	428	0	23	1157	640	8.569	0	28	75.3	76.70	1.86

SP: Superplasticizer
 VMA: Viscosity Modifying Agent
 E (%): Relative percentage error

The model has a neural network architecture with nine input variables, one output variable, and one hidden layer with 25 nodes as indicated in Figure 2 while the values of its statistical indexes including the R², MAPE, and RMSE are listed in Table 6.

The actual values and those predicted by the best BPNN model were compared using the two graphs presented in Figure 3 and the suggested optimal 9-25-1 model was observed to have the capacity to correctly forecast the industrial waste incorporated SCC’s compressive strength with a small er-

ror margin. It is worth noting that the variation of almost every sample utilized in the testing procedure is less than ±10% as indicated in Figure 4.

Figure 4 shows the overall performance of the ANN in forecasting the strength in all ages while Figures 5 to 8 indicate the performance at 7, 28, 90, and 180-day periods respectively. It was discovered from the results that most points are within the ±10% lines and this means the networks can accurately predict SCC strength. Moreover, the overall correlation coefficient of the model was 0.9835

which is very high and also has a smaller RMSE value of 2.4503 compared to other similar studies (Nguyen et al., 2020; Uysal and Tanyildizi, 2011).

The final trained model recalled the data not used in the training phase which include 354 mixes in order to evaluate the accuracy of the ANN model. A total of 16 unknown combinations were also presented to the model developed within the training data sets range to predict the output in the form of the SCC strength.

Table 7 shows the proportion of mixtures as well as the measured and predicted values.

3.1 Parametric analysis of developed ANN model

Parametric analysis of a model is a technique usually used to identify the influence of alterations

in the input assumptions on the output (Grady, 2014) and this is considered important. This analysis also makes it possible to understand the level of sensitivity of the input variables to determine those that are more important. Furthermore, the removal of inconsequential variables reduces the input space, leading to a decrease in the complication of the network and the necessary time for training. The analysis was applied to test the sensitivity of the input parameters. It was achieved by determining the effect of altering one parameter while all others are kept constant. Therefore, some key input variables were assessed to establish the functional relationships between the mixture variables and the compressive strength.

3.1.1 Effect of fly ash

Different amounts of fly ash were used to replace cement content while other parameters are kept

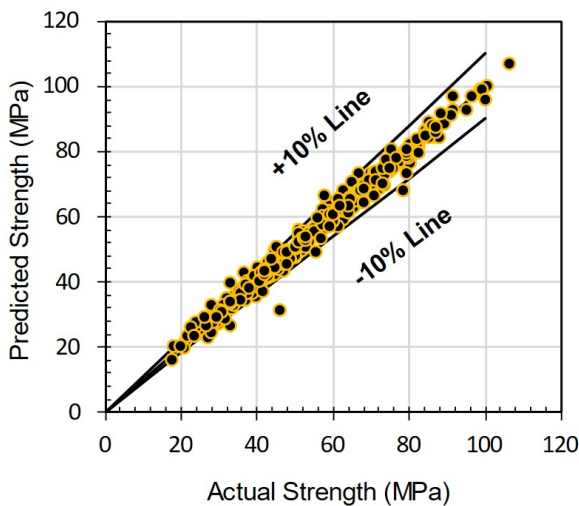


Figure 4. Actual v/s predicted strength for all ages

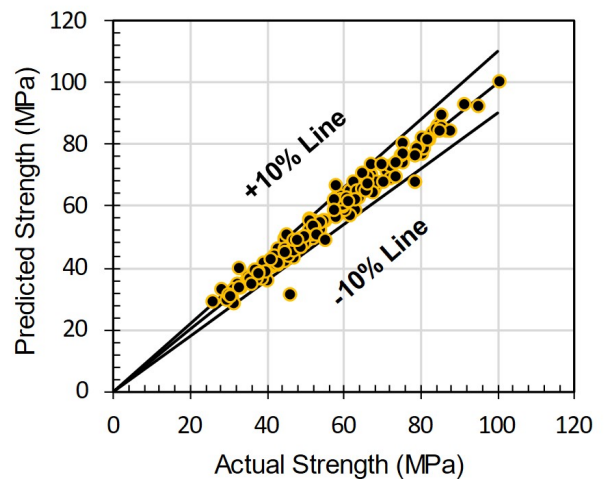


Figure 6. Actual v/s predicted strength for 28-days

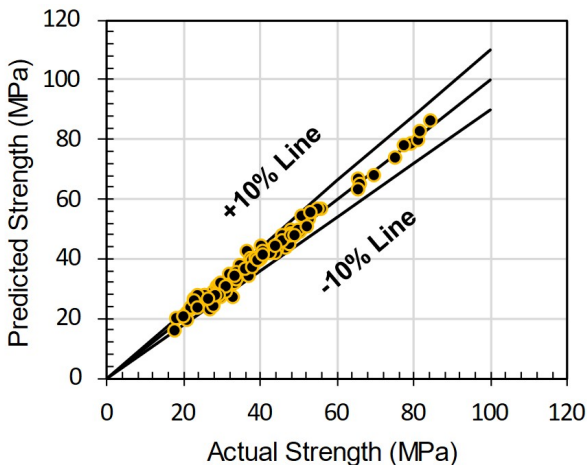


Figure 5. Actual v/s predicted strength for 7-days

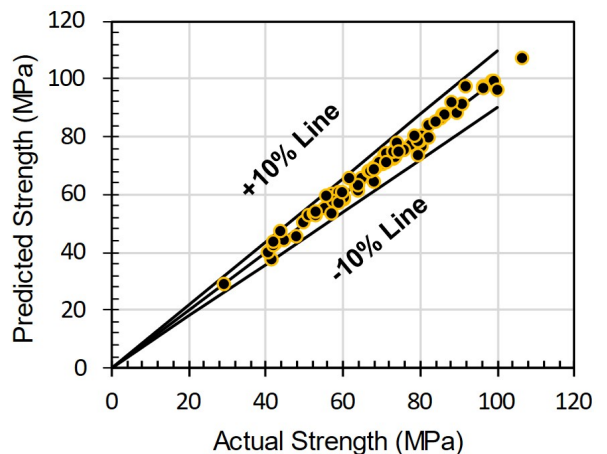


Figure 7. Actual v/s predicted strength for 90-days

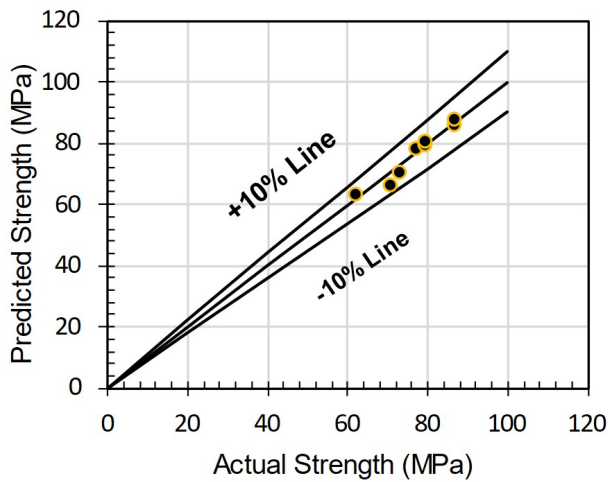


Figure 8. Actual v/s predicted strength for 180-days

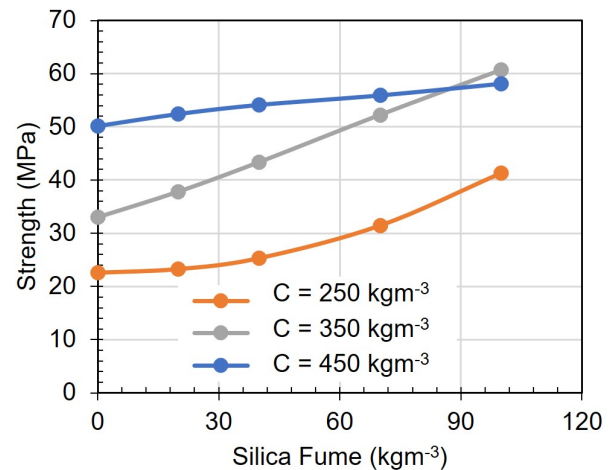


Figure 10. Silica fume impact on SCC strength

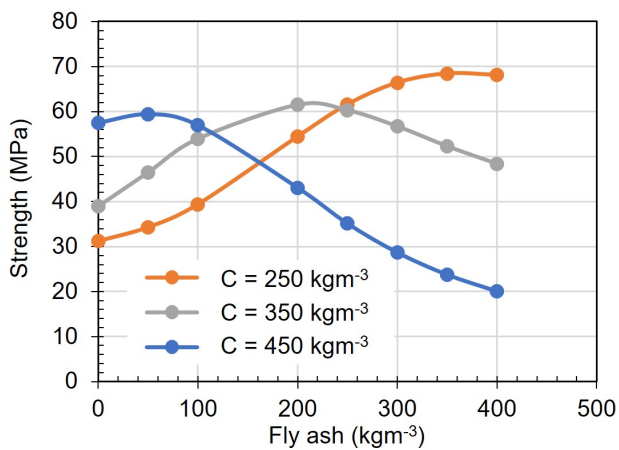


Figure 9. Impact of fly ash on strength

constant to evaluate its sensitivity to the compressive strength. Figure 9 shows that the replacement level of fly ash has a considerable impact on the strength. It was discovered that an increase in its quantity up to the optimum level of replacement for the cement led to an increment in the compressive strength (28-day) after which the strength reduced. This means an increase in the amount of fly ash after its optimum level as a replacement material directly correlates with the reduction in strength. Similar results have also been found in previously published studies (Ahmad et al., 2020; Naik et al., 2012). This is associated with the pozzolanic reaction of aluminosilicate oxides in fly ash with calcium hydroxide which generates additional cementitious compounds and allows the concrete containing fly ash to gain strength over time. However, the total cement and fly ash content over 550 kgm^{-3} was generally found to be at an optimum range of total binder. This was fol-

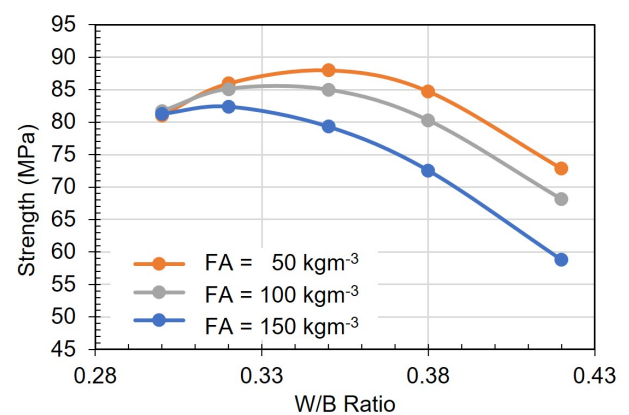


Figure 11. Effect of w/b ratio

lowed by the replacement of the fine aggregates by the cement content which subsequently interferes with the water demand and packing of the matrix (Chandra and Bendapudi, 2015).

3.1.2 Effect of silica fume

Silica fume also has a considerable impact on the strength of SCC and this was observed by changing its quantity while other parameters were kept constant to evaluate its impact. The compressive strength (28-day) was observed to have increased with the amount of silica fume as indicated in Figure 10 from 0 to 130 kg replacement and different cement content. This has also been confirmed in previous studies (Turk et al., 2012).

The trend is due to the fact silica fume is a very active and very fine mineral additive that enhances the bond between fine aggregate and the hydrated cement in concrete mix within a short period. In addition, the unreacted material fills the very

fine pores in the matrix (Moghadam and Izadifard, 2019) and all these mechanisms increase the compressive strength of SCC.

3.1.3 Effect of w/b ratio

Water-binder ratio is one of the most important parameters for any kind of concrete due to its direct relationship with the compressive strength. This was notably true when making highly workable self-compacting concrete with a large amount of paste which frequently leads to a greater w/b ratio (Neville, 2011). Figure 11 shows the change in strength due to the w/b ratio for different amounts of fly ash after 28-days. The combined effects of the increase in the amount of fly ash and w/b ratio were observed to have led to the reduction in the strength after the optimum level of fly ash as been reached at 28-days. This phenomenon has been previously discussed by Siddique (2011).

The strength of concrete depends on its porosity and hydration reaction also requires a minimum amount of water. Meanwhile, more water increases the w/b ratio, dilutes cement paste, and increases the water-filled pore space between the particles (Beaudoin and Odler, 2019). This requires the hydrates to grow larger in order to interact and improve strength and fill the gap between them. This simply means any extra water beyond the hydration requirement is expected to produce more capillary pores, thereby reducing the area of solid hydrates for the same cross-sectional area of concrete and lowering the strength. Sometimes, desirable workability can be achieved with a lower

w/b ratio by using a superplasticizer but the application of too much superplasticizer can also affect the ultimate strength (Islam et al., 2019).

3.1.4 Effect of superplasticizer

Superplasticizer is very important to the improvement of the rheological characteristics of SCC and this means it is a necessary component for the production process. Figure 12 shows the change in strength due to varying SP dosages from 4 to 12 kg with different amounts of fly ash from 50 to 150 kg at 28-days.

The increase in the FA and superplasticizer was observed to have led to the reduction of the SCC strength at 28-days. For a given flowability, the superplasticizer has the ability to enhance strength by reducing mixed water or lowering both water and cement content to reach the desired flowability and strength (Aïtcin, 1995). Meanwhile, the production of self-compacting concrete using only Portland cement allows the fly ash to lower the amount of the superplasticizer required to achieve equivalent strength (Naik et al., 2012). It is important to note that the superplasticizer with cement and with fly ash does not have the same work mechanism. This is the reason an increase in the superplasticizer content based on total cementitious binder negatively affected the strength but a minor difference was noted with a change in the fly ash content.

The situation was different with silica fume as indicated in Figure 13 where the 28-day compressive

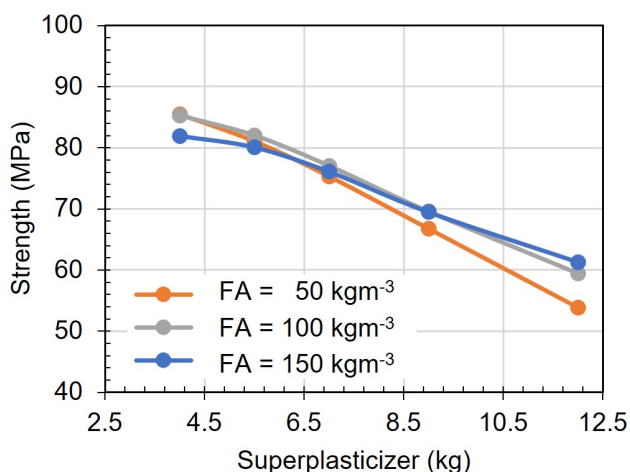


Figure 12. Effect of SP with fly ash

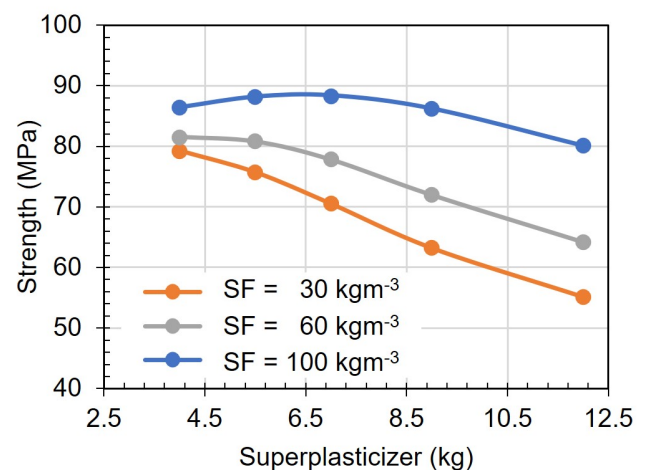


Figure 13. Effect of SP with silica fume

Table 8. Parameters for spreadsheet calculation

Parameters	Description
p_1	Input matrix (9x1)
$LW_{1,1}$	Weight matrix between input and hidden layer (25x9)
b_1	Bias matrix of the hidden layer (25x1)
x_{p1}	Normalization of input values (9x1)
a_1	Tansig function values (matrix) of n_1 (25x1)
$LW_{2,1}$	Weight matrix between hidden and output layer (1x25)
b_2	Bias matrix of the output layer (1x1)
y	Output matrix (1x1)

strength changes at different SP dosages from 4 to 12 kg for various silica fume concentrations. This is due to the fact that silica fume, as the finest material, generally demands more water (Levy, 2012). This means increasing the superplasticizer content has the ability to improve the situation when there is low water content, specifically when a higher amount of silica fume was used in the matrix. However, an increase in the concentration beyond an optimum level can have a negative influence on the 28-day strength (Neville, 2011) due to the addition of more water to the concrete. An increased amount of superplasticizer leads to bleeding and segregation with a subsequent effect on the cohesiveness and homogeneity of the SCC, thereby leading to a decrease in its strength (Aicha, 2020).

3.2 Practical implication

Practical engineers and users require tools or programs to predict the strength of concrete rather than just an ANN architecture. This can be achieved through the design and production of a ready-made tool for the calculation.

It is possible to develop a spreadsheet program using the weights, biases, and other parameters obtained from the trained network using the process summarized in Figure 15 and the parameters described in Table 8. The whole procedure is outlined as follows.

1. Normalize the input matrix (p_1) value using the following equation – For every input variable,

$$x_{p1} = [(p_1 - offset) \times gain] + x_{min} \quad (4)$$

Where, as listed in Table 9.

Table 9. Parameters for spreadsheet calculation

X_{offset}	X_{gain}	X_{min}
0.3	13.33333333	-1
135	0.004123711	-1
0	0.004761905	-1
0	0.013333333	-1
657	0.003929273	-1
590	0.004878049	-1
0.585	0.151343171	-1
0	0.496277916	-1
7	0.011560694	-1

SCC Strength using ANN			
Input			Output
Mix Proportion	Range (kg/m3)	Amount (kg/m3)	Compressive Strength (MPa)
W/B Ratio	(0.3 - 0.45)	0.37	45.987
Cement	(135 - 600)	500	
Fly Ash	(0 - 420)	100	
Silica Fume	(0 - 150)	25	
Fine Agg.	(657 - 1166)	890	
Coarse Agg.	(590 - 1000)	900	
SP	(0.585 - 13.8)	7.8	
VMA	(0 - 4.03)	0	
Age	(7 - 180) days	28	

Figure 14. Spreadsheet for predicting SCC strength

2. Find the multiplication matrix value (n_1) of the normalized input matrix with $LW_{1,1}$ and add the multiplied value with b_1 using Equation (5).

$$n_1 = (x_{p1} \times LW_{1,1}) + b_1 \quad (5)$$

3. Calculate hyperbolic tangent sigmoid transfer function's (tansig) matrix value using Equation (6). For each value of n_1 .

$$a_1 = \left[\frac{2}{1 + \exp(-2 \times n_1)} \right] - 1 \quad (6)$$

4. Using Equation (7), calculate the multiplication matrix (n_2) value of the tansig function matrix and $LW_{2,1}$ and add the multiplied value with b_2 .

$$n_2 = (a_1 \times LW_{2,1}) + b_2 \quad (7)$$

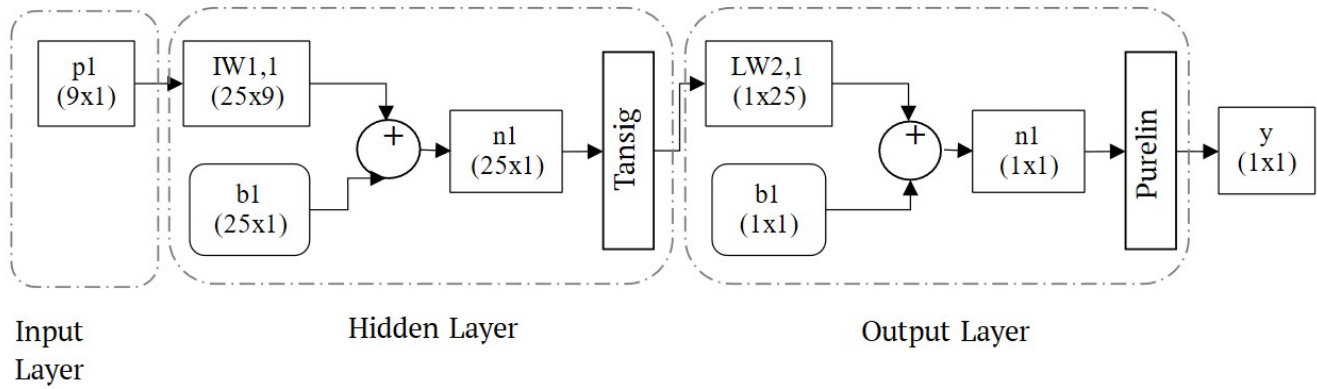


Figure 15. Network diagram

5. Finally, calculate the output value (y) by reversing the normalized value using Equation (8).

$$y = \left(\frac{n_2 - y_{\min}}{y_{\text{gain}}} \right) + y_{\text{offset}} \quad (8)$$

Where,

$$\begin{aligned} y_{\min} &= -1 \\ y_{\text{gain}} &= 0.0224971878515186 \\ y_{\text{offset}} &= 17.7 \end{aligned} \quad (9)$$

4 CONCLUSION

The main goal of the paper was to develop an optimum BPNN model and to develop a procedure to create a tool or program for practical uses. Following the goal, a network architecture is developed which can reliably predict the strength of SCC. The proposed neural network architecture can make a reliable prediction as the trained network obtained very low RMSE (2.4503) and MAPE (0.0347) values. Also, the higher R^2 (0.9835) value is obtained, making the predicted values very similar to actual values. The developed network can also assess the sensitivity or influence of individual parameters using parametric analysis. The impact of individual parameters on the compressive of SCC was significant. The sensitivity result agrees with the previously published studies. An approach to creating a spreadsheet program for practical users is proposed. Moreover, the proposed procedures of creating a spreadsheet program can be used by field engineers and users directly, which would be very handy and fast to predict the strength of self-compacting concrete. Although the model predic-

tion is limited to its boundary limits (ranges of input parameters), it can be easily retrained with a broader scope by utilizing the proposed optimum neural network model.

DISCLAIMER

The authors declared that they have no known competing financial interests or personal relationships that could have appeared to influence the work reported in this paper.

ACKNOWLEDGMENTS

The laboratory's support from the Department of Civil Engineering, Chittagong University of Engineering Technology (CUET) is greatly acknowledged.

REFERENCES

- Ahmad, J., Ihsan, M. T., Manan, A., Zaid, O., Ullah, R. and Abbas, G. (2020), 'Evaluating the effect of fly ash on the rheological and mechanical performance self-compacted concrete', p. 10.
- Aicha, M. B. (2020), The superplasticizer effect on the rheological and mechanical properties of self-compacting concrete, in 'New Materials in Civil Engineering', Elsevier, pp. 315–331.
URL: <https://doi.org/10.1016/b978-0-12-818961-0.00008-9>
- Al-Hadithi, A. I. and Hilal, N. N. (2016), 'The possibility of enhancing some properties of self-compacting concrete by adding waste plastic

fibers', *Journal of Building Engineering* **8**, 20–28.
URL: <https://doi.org/10.1016/j.jobbe.2016.06.011>

American Concrete Institute (2019), 'Aci prc-237-07 self-consolidating concrete', p. 30.
URL: www.concrete.org/store/productdetail.aspx?ItemID=23707Format=DOWNLOADLanguage=EnglishUnits=US_AND_METRIC

Apostolopoulou, M., Armaghani, D. J., Bakolas, A., Douvika, M. G., Moropoulou, A. and Asteris, P. G. (2019), 'Compressive strength of natural hydraulic lime mortars using soft computing techniques', *Procedia Structural Integrity* **17**, 914–923.
URL: <https://doi.org/10.1016/j.prostr.2019.08.122>

Armaghani, D. J., Hatzigeorgiou, G. D., Karamani, C., Skentou, A., Zoumpoulaki, I. and Asteris, P. G. (2019), 'Soft computing-based techniques for concrete beams shear strength', *Procedia Structural Integrity* **17**, 924–933.
URL: <https://doi.org/10.1016/j.prostr.2019.08.123>

Ashteyat, A. A. and Ismeik, M. (2018), 'Predicting residual compressive strength of self-compacted concrete under various temperatures and relative humidity conditions by artificial neural networks', *Computers and Concrete*, *21*(1) p. 47.
URL: <https://doi.org/10.12989/CAC.2018.21.1.047>

Asteris, P. G., Apostolopoulou, M., Skentou, A. D. and Moropoulou, A. (2019a), 'Predicting application of artificial neural networks for the prediction of the compressive strength of cement-based mortars', *Computers and Concrete*, *24*(4) p. 329.
URL: <https://doi.org/10.12989/CAC.2019.24.4.329>

Asteris, P. G., Armaghani, D. J., Hatzigeorgiou, G. D., Karayannis, C. G. and Pilakoutas, K. (2019b), 'Predicting the shear strength of reinforced concrete beams using artificial neural networks', *Computers and Concrete*, *24*(5) p. 469.
URL: <https://doi.org/10.12989/CAC.2019.24.5.469>

Asteris, P. G., Tsaris, A. K., Cavaleri, L., Repapis, C. C., Papalou, A., Trapani, F. D. and Karypidis, D. F. (2016), 'Prediction of the fundamental period of infilled RC frame structures using artificial neural networks', *Computational Intelligence and Neuroscience* **2016**, 1–12.
URL: <https://doi.org/10.1155/2016/5104907>

Aïtcin, P.-C. (1995), 'Developments in the application of high-performance concretes', *Construction and Building Materials* **9**(1), 13–17.

URL: [https://doi.org/10.1016/0950-0618\(95\)92855-b](https://doi.org/10.1016/0950-0618(95)92855-b)

Banthia, N. and Onuaguluchi, O. (2021), 'Recycling scrap tire-derived fibers in concrete', *Transactions of the Indian National Academy of Engineering* **7**(1), 207–217.
URL: <https://doi.org/10.1007/s41403-021-00257-4>

Beaudoin, J. and Odler, I. (2019), Hydration, setting and hardening of portland cement, in 'Lea's Chemistry of Cement and Concrete', Elsevier, pp. 157–250.
URL: <https://doi.org/10.1016/b978-0-08-100773-0.00005-8>

Cavaleri, L., Chatzarakis, G. E., Trapani, F. D., Douvika, M. G., Roinos, K., Vaxevanidis, N. M. and Asteris, P. G. (2017), 'Modeling of surface roughness in electro-discharge machining using artificial neural networks', *Advances in Materials Research (South Korea)*, *6*(2) p. 169–184.
URL: <https://doi.org/10.12989/amr.2017.6.2.169>

Chandra, S. and Bendapudi, K. (2015), 'Contribution of fly ash to the properties of mortar and concrete', *International Journal of Earth Sciences and Engineering*, *04*(October 2011) p. 1017–1023.

Chugh, A. (2020), 'Coefficient of determination, adjusted r squared – which metric is better?'.
URL: <https://medium.com/analytics-vidhya/mae-mse-rmse-coefficient-of-determination-adjusted-r-squared-which-metric-is-better-cd0326a5697e>

Deilami, S., Aslani, F. and Elchalakani, M. (2017), 'Durability assessment of self-compacting concrete with fly ash', *Computers and Concrete*, *19*(5) p. 489.
URL: <https://doi.org/10.12989/CAC.2017.19.5.489>

Grünewald, S. and Walraven, J. C. (2001), 'Parameter-study on the influence of steel fibers and coarse aggregate content on the fresh properties of self-compacting concrete', *Cement and Concrete Research* **31**(12), 1793–1798.
URL: [https://doi.org/10.1016/s0008-8846\(01\)00555-5](https://doi.org/10.1016/s0008-8846(01)00555-5)

Heniegal, A. M. (2012), 'Numerical analysis for predicting of self compacting concrete mixtures using artificial neural networks', *JES. Journal of Engineering Sciences* **40**(6), 1575–1597.
URL: <https://doi.org/10.21608/jesaun.2012.114530>

Hinton, G. E., Osindero, S. and Teh, Y.-W. (2006), 'A fast learning algorithm for deep belief nets', *Neural Computation* **18**(7), 1527–1554.

URL: <https://doi.org/10.1162/neco.2006.18.7.1527>

Hodhod, O. A., Said, T. E. and Ataya, A. M. (2018), 'Prediction of creep in concrete using genetic programming hybridized with ann', *Computers and Concrete*, **21**(5) p. 513.

URL: <https://doi.org/10.12989/CAC.2018.21.5.513>

Hornik, K., Stinchcombe, M. and White, H. (1989), 'Multilayer feedforward networks are universal approximators', *Neural Networks* **2**(5), 359–366.

URL: [https://doi.org/10.1016/0893-6080\(89\)90020-8](https://doi.org/10.1016/0893-6080(89)90020-8)

Intezar, T. M., Haque, S., Islam, G. M. S. and Roy, S. and Mushfiq, M. (2019), 'Properties of self-compacting concrete using fly ash and polypropylene fibre', *5th International Conference on Engineering Research, Innovation and Education ICERIE 2019*.

Islam, G. M. S., Raihan, M. T., Hasan, M. M. and Rashadin, M. (2019), 'Effect of retarding superplasticizers on the properties of cement paste, mortar and concrete', *Asian Journal of Civil Engineering* **20**(4), 591–601.

URL: <https://doi.org/10.1007/s42107-019-00128-y>

Joshi, R. C. and Lohtia, R. P. (1997), 'Fly ash in concrete, production, properties and uses', *Advances in Concrete technology (Volume 2)*.

Lee, S. C. and Han, S. W. (2002), 'Neural-network-based models for generating artificial earthquakes and response spectra', *Computers & Structures* **80**(20-21), 1627–1638.

URL: [https://doi.org/10.1016/s0045-7949\(02\)00112-8](https://doi.org/10.1016/s0045-7949(02)00112-8)

Lee, S. C., Park, S. K. and Lee, B. H. (2001), 'Development of the approximate analytical model for the stub-girder system using neural networks', *Computers & Structures* **79**(10), 1013–1025.

URL: [https://doi.org/10.1016/s0045-7949\(00\)00199-1](https://doi.org/10.1016/s0045-7949(00)00199-1)

Levy, S. M. (2012), Calculations relating to concrete and masonry, in 'Construction Calculations Manual', Elsevier, pp. 211–264.

URL: <https://doi.org/10.1016/b978-0-12-382243-7.00005-x>

Lourakis, M. (2005), 'A brief description of the levenberg-marquardt algorithm implemented by levmar', *Matrix*, **3**(January 2005) p. 2.

Mazloom, M., Soltani, A., karamloo, M., Hassanloo, A. and Ranjbar, A. (2018), 'Effects of silica fume, superplasticizer dosage and type of superplasticizer on the properties of normal and self-compacting concrete', *Advances in Materials Research*, **7**(1) p. 45.

URL: <https://doi.org/10.12989/AMR.2018.7.1.045>

Mazloom, M. and Yoosefi, M. M. (2013), 'Predicting the indirect tensile strength of self-compacting concrete using artificial neural networks', *Computers and Concrete*, **12**(3) p. 285.

URL: <https://doi.org/10.12989/CAC.2013.12.3.285>

McCarthy, M. J., Islam, G. M. S., Csetenyi, L. J. and Jones, M. R. (2013), 'Evaluating test methods for rapidly assessing fly ash reactivity for use in concrete', *World of Coal Ash Conference, April 22-25*.

Moghadam, M. A. and Izadifard, R. A. (2019), 'Experimental investigation on the effect of silica fume and zeolite on mechanical and durability properties of concrete at high temperatures', *SN Applied Sciences* **1**(7).

URL: <https://doi.org/10.1007/s42452-019-0739-2>

Mohammadhosseini, H. and Yatim, J. M. (2017), 'Evaluation of the effective mechanical properties of concrete composites using industrial waste carpet fiber', *INAE Letters* **2**(1), 1–12.

URL: <https://doi.org/10.1007/s41403-017-0016-x>

Naik, T. R., Kumar, R., Ramme, B. W. and Canpolat, F. (2012), 'Development of high-strength, economical self-consolidating concrete', *Construction and Building Materials* **30**, 463–469.

URL: <https://doi.org/10.1016/j.conbuildmat.2011.12.025>

Neville, A. M. (2011), *Properties of Concrete (5th ed.)*. Pearson Education Limited.

Nguyen, T. T., Duy, H. P., Thanh, T. P. and Vu, H. H. (2020), 'Compressive strength evaluation of fiber-reinforced high-strength self-compacting concrete with artificial intelligence', *Advances in Civil Engineering* **2020**, 1–12.

URL: <https://doi.org/10.1155/2020/3012139>

Nikoo, M., Sadowski, Ł., Khademi, F. and Nikoo, M. (2017), 'Determination of damage in reinforced concrete frames with shear walls using self-organizing feature map', *Applied Computational Intelligence and Soft Computing* **2017**, 1–10.

URL: <https://doi.org/10.1155/2017/3508189>

Okamura, H. and Ouchi, M. (2003), 'Self-compacting concrete', *Journal of Advanced Concrete Technology* **1**(1), 5–15.

URL: <https://doi.org/10.3151/jact.1.5>

Raheman, A. and Modani, P. O. (2013), *Prediction of Properties of Self Compacting Concrete Using Artificial Neural Network*. **3**(4) pp. 333–339.

Saini, G. and Vattipalli, U. (2020), 'Assessing properties of alkali activated GGBS based self-compacting geopolymer concrete using nano-silica', *Case Studies in Construction Materials* **12**, e00352.

URL: <https://doi.org/10.1016/j.cscm.2020.e00352>

Schmidhuber, J. (2015), 'Deep learning in neural networks: An overview', *Neural Networks* **61**, 85–117.

URL: <https://doi.org/10.1016/j.neunet.2014.09.003>

Siddique, R. (2011), 'Properties of self-compacting concrete containing class f fly ash', *Materials & Design* **32**(3), 1501–1507.

URL: <https://doi.org/10.1016/j.matdes.2010.08.043>

Siddique, R., Aggarwal, P., Aggarwal, Y. and Gupta, S. M. (2008), 'Modeling properties of self-compacting concrete: support vector machines

approach', *Computers and Concrete*, **5**(5) p. 461.

URL: <https://doi.org/10.12989/CAC.2008.5.5.461>

Taylor, J. G., ed. (1992), *Neural Network Applications*, Springer London.

URL: <https://doi.org/10.1007/978-1-4471-2003-2>

Turk, K., Karatas, M. and Gonen, T. (2012), 'Effect of fly ash and silica fume on compressive strength, sorptivity and carbonation of SCC', *KSCE Journal of Civil Engineering* **17**(1), 202–209.

URL: <https://doi.org/10.1007/s12205-013-1680-3>

Uysal, M. and Tanyildizi, H. (2011), 'Predicting the core compressive strength of self-compacting concrete (SCC) mixtures with mineral additives using artificial neural network', *Construction and Building Materials* **25**(11), 4105–4111.

URL: <https://doi.org/10.1016/j.conbuildmat.2010.11.108>

Vandeput, N. (2019), 'Forecast kpi: Rmse, mae, mape bias | towards data science.'

URL: <https://towardsdatascience.com/forecast-kpi-rmse-mae-mape-bias-cdc5703d242d>

Yadollahi, M. M., Benli, A. and Demirboğa, R. (2015), 'Prediction of compressive strength of geopolymer composites using an artificial neural network', *Materials Research Innovations* **19**(6), 453–458.

URL: <https://doi.org/10.1179/1433075x15y.0000000020>

Ye, X. W., Jin, T. and Yun, C. B. (2019), 'A review on deep learning-based structural health monitoring of civil infrastructures', *Smart Structures and Systems*, **24**(5) p. 567.

URL: <https://doi.org/10.12989/SSS.2019.24.5.567>

[This page is intentionally left blank]